

Supplementary Materials for
Sulfated bile acid is a host-derived ligand for MAIT cells

Emi Ito *et al.*

Corresponding author: Sho Yamasaki, yamasaki@biken.osaka-u.ac.jp

Sci. Immunol. **9**, eade6924 (2024)
DOI: 10.1126/sciimmunol.ade6924

The PDF file includes:

Materials and Methods
Figs. S1 to S7
Tables S1 to S4
Legend for data S1
References (85–90)

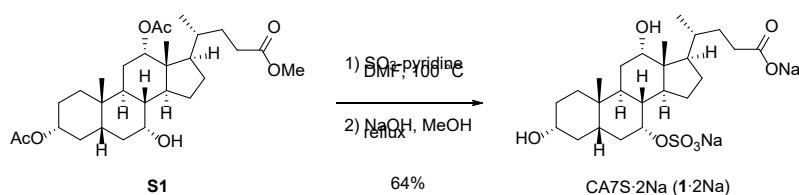
Other Supplementary Material for this manuscript includes the following:

Data S1
MDAR Reproducibility Checklist

SUPPLEMENTARY MATERIALS AND METHODS

General methods for the synthesis of compounds

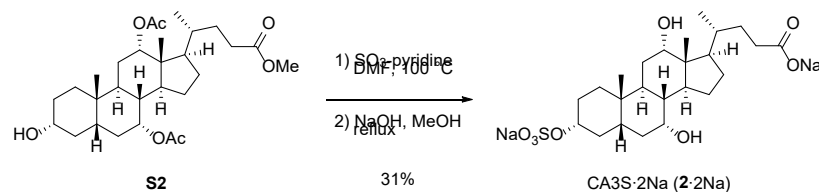
^1H NMR spectra were recorded using a JEOL ECA-500 or JEOL ECZ600R spectrometer. Chemical shifts are reported in δ (ppm) relative to Me_4Si (in CDCl_3 and CD_3OD) and MeCN signal (in D_2O) as internal standards. ^{13}C NMR spectra were recorded using a JEOL ECA-500 or JEOL ECZ600R spectrometer and referenced to the residual CHCl_3 signal (in CDCl_3), CD_3OD signal (in CD_3OD) and MeCN signal (in D_2O). IR spectra were obtained on a JASCO FT/IR-4100 spectrometer. High-resolution mass spectrometry (HRMS) spectra were recorded on a Shimadzu LC-ESI-IT-TOF-MS equipment (ESI). Optical rotations were measured with a JASCO P-1020 polarimeter. Column chromatography was performed using flash chromatography on a Wakogel C-300E (Wako). For thin-layer chromatography, a silica gel 70 F₂₅₄ plate was employed. Compounds CA7S (Compound 1) (85), CA3S (Compound 2) (85, 86), CA12S (Compound 3) (85), TCA7S (Compound 4) (85), S7 (85), and S9 (85) are known and were synthesized by modifying previously published methods. Compounds TCA3S (Compound 7) (85, 86), S1 (87), S2 (86), S3 (88), S8 (85) and RL-7-Me (24) were also previously described and were prepared according to the previously published methods.



Disodium cholate 7-sulfate (CA7S·2Na)

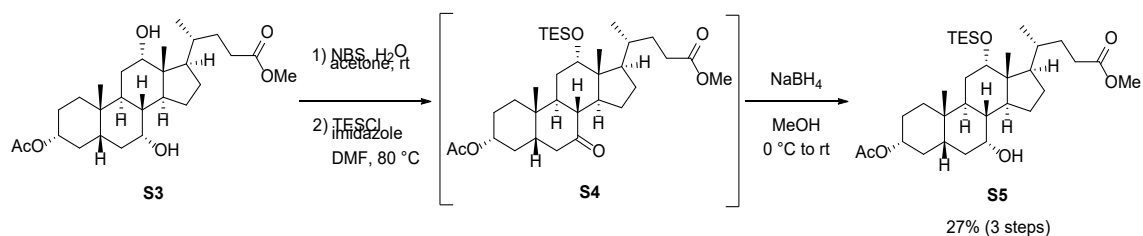
CA7S·2Na was synthesized by modifying of a previously published method (89, 90). Sulfur trioxide-pyridine complex (565 mg, 3.54 mmol) was added to a stirred solution of Compound S1 (179 mg, 0.352 mmol) in dry DMF (2 ml) under an argon atmosphere. After 24 hours of

constant stirring at 100°C, the mixture was concentrated in vacuo. The residue was dissolved in a solution of NaOH (0.493 g, 12.3 mmol) in MeOH (10 ml). After 18 hours of constant stirring at 90°C, the mixture was adjusted to pH 8 with 10% aqueous HCl and concentrated in vacuo. MeOH was added to the residue and the resulting precipitate was filtered. After the filtrate was concentrated in vacuo, the residue was dissolved in water (5 ml), which was purified by Sep-Pak[®] C18 cartridge. The cartridge was activated by MeOH and equilibrated by water before loading. After the residue was loaded and desalinated by water (10 ml), the product was eluted by 20% MeCN aq. (20 ml, four times). The eluent was lyophilized to yield CA7S·2Na (Compound 1·2Na) as a white solid (119 mg, 64%). NMR measurements were performed after dissolving the product in 20% MeCN aq. containing 0.1% TFA followed by lyophilization: mp 173–174°C; $[\alpha]^{25}_D +10.6$ (*c* 0.700, MeOH); IR (neat cm^{-1}): 3336 (OH), 1559 (C=O), 1412 (S=O); ^1H NMR (600 MHz, D_2O) δ 0.73 (s, 3H), 0.93 (s, 3H), 0.97 (d, *J* = 6.9 Hz, 3H), 1.00–1.07 (m, 1H), 1.08–1.16 (m, 1H), 1.25–1.41 (m, 3H), 1.42–1.53 (m, 2H), 1.56–1.61 (m, 1H), 1.61–1.71 (m, 3H), 1.71–1.98 (m, 8H), 1.92–1.98 (m, 1H), 1.99–2.10 (m, 2H), 2.32 (ddd, *J* = 15.1, 9.0, 7.5 Hz, 1H), 2.45 (ddd, *J* = 15.1, 9.8, 5.5 Hz, 1H), 3.49–3.55 (m, 1H), 4.05–4.08 (m, 1H), 4.49–4.52 (m, 1H); $^{13}\text{C}\{^1\text{H}\}$ NMR (150 MHz, D_2O) δ 12.5, 17.1, 22.4, 23.1, 27.59, 27.62, 28.1, 29.8, 31.0, 31.3, 31.7, 34.5, 35.0, 35.4, 38.4, 39.3, 41.4, 42.1, 46.7, 47.1, 72.2, 73.8, 80.1, 180.8; HRMS (ESI-TOF) *m/z*: $[\text{M} + \text{H} - 2\text{Na}]^-$ calculated for $\text{C}_{24}\text{H}_{39}\text{O}_8\text{S}$, 487.2371; found, 487.2379.



Disodium cholate 3-sulfate (CA3S·2Na)

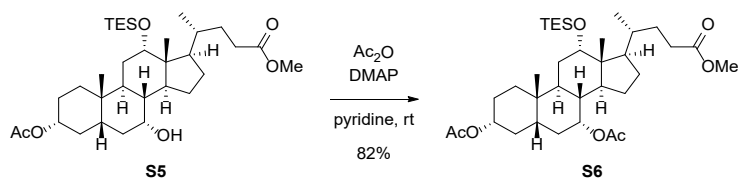
Using a procedure identical with that described for synthesis of Compound 1·2Na from Compound S1, cholic acid derivative Compound S2 (100 mg, 0.197 mmol) was converted into CA3S·2Na (Compound 2·2Na) as a white solid (32.5 mg, 31%): mp 193–195°C; $[\alpha]^{25}_D +33.8$ (*c* 0.405, MeOH); IR (neat cm^{-1}): 3369 (OH), 1565 (C=O), 1409 (S=O); ^1H NMR (500 MHz, D_2O) δ 0.72 (s, 3H), 0.93 (s, 3H), 0.97 (d, $J = 6.9$ Hz, 3H), 1.02–1.10 (m, 1H), 1.11–1.21 (m, 1H), 1.25–1.36 (m, 2H), 1.38–1.46 (m, 1H), 1.47–1.58 (m, 3H), 1.58–1.62 (m, 1H), 1.62–1.71 (m, 4H), 1.71–1.81 (m, 2H), 1.81–1.94 (m, 4H), 1.99–2.04 (m, 1H), 2.07–2.14 (m, 2H), 2.17–2.27 (m, 2H), 3.89–3.91 (m, 1H), 4.06–4.08 (m, 1H), 4.18–4.24 (m, 1H); $^{13}\text{C}\{^1\text{H}\}$ NMR (125 MHz, D_2O) δ 12.5, 17.3, 22.3, 23.3, 26.9, 27.7, 28.0, 28.1, 32.9, 34.1, 34.8, 35.0, 35.3, 35.8, 36.7, 39.5, 41.6, 42.2, 46.7, 47.4, 69.1, 74.0, 82.1, 185.3; HRMS (ESI-TOF) m/z : $[\text{M} + \text{H} - 2\text{Na}]^-$ calculated for $\text{C}_{24}\text{H}_{39}\text{O}_8\text{S}$, 487.2371; found, 487.2376.



Compound S5

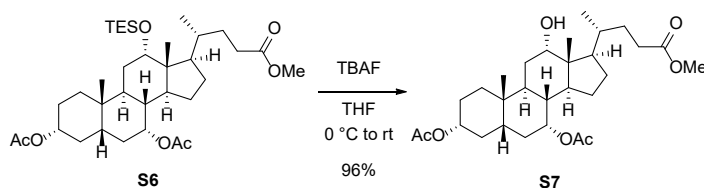
NBS (1.40 g, 7.85 mmol) was added to a stirred solution of Compound S3 (2.92 g, 6.28 mmol) in water (39 ml) and acetone (56 ml) at room temperature. After 16 hours of constant stirring at this temperature, the mixture was concentrated in vacuo, and the residue was dissolved in CH_2Cl_2 . The organic layer was washed with brine, dried over Na_2SO_4 , and concentrated in vacuo to yield a crude product (1.73 g). Imidazole (1.54 g, 22.7 mmol) and chlorotriethylsilane (2.52 ml, 15.0 mmol) were then added to a solution of the crude product (1.73 g) in dry DMF

(9.3 ml) at room temperature. After constant stirring for 3 hours at 80°C under an argon atmosphere, the mixture was diluted with MeOH and concentrated in vacuo. The residue was dissolved in EtOAc, washed with brine, and dried over Na₂SO₄. After concentration in vacuo, the residue was purified by flash chromatography over silica gel with *n*-hexane–EtOAc (7:1 to 5:1) to yield a ketone, Compound S4, which was used without further purification. NaBH₄ (192 mg, 5.08 mmol) was added to a solution of the ketone Compound S4 in MeOH (16 ml) at 0°C. After constant stirring for 2 hours at room temperature, the mixture was diluted with saturated aqueous NH₄Cl. The whole mixture was extracted with Et₂O and dried over Na₂SO₄. After concentration in vacuo, the residue was purified by flash chromatography over silica gel with *n*-hexane–EtOAc (6:1 to 4:1) to yield Compound S5 as a white amorphous solid (957 mg, 27% over three steps): mp 43–44°C; [α]_D²⁵ +46.7 (*c* 0.473, CHCl₃); IR (neat cm⁻¹): 3543 (OH) 1728 (C=O); ¹H NMR (500 MHz, CDCl₃) δ 0.63 (q, *J* = 8.0 Hz, 6H), 0.66 (s, 3H), 0.90 (s, 3H), 0.96 (d, *J* = 6.3 Hz, 3H), 0.99–1.15 (m, 2H), 1.00 (t, *J* = 8.0 Hz, 9H), 1.20–1.40 (m, 4H), 1.42–1.55 (m, 6H), 1.57–1.65 (m, 1H), 1.65–1.75 (m, 2H), 1.76–1.86 (m, 2H), 1.87–1.96 (m, 3H), 1.97–2.05 (m, 1H), 2.01 (s, 3H), 2.18–2.34 (m, 3H), 2.37 (ddd, *J* = 15.5, 10.3, 5.2, 1H), 3.67 (s, 3H), 3.82–3.85 (m, 1H), 4.03–4.06 (m, 1H), 4.52–4.60 (m, 1H); ¹³C {¹H} NMR (125 MHz, CDCl₃) δ 5.8 (3C), 7.3 (3C), 12.4, 17.6, 21.5, 22.7, 23.4, 26.6, 26.8, 27.8, 28.9, 31.0, 31.1, 34.1, 34.87, 34.93, 35.4, 35.7 39.8, 41.2, 41.3, 46.1, 47.2, 51.5, 68.4, 73.8, 74.2, 170.9, 174.7; HRMS (ESI-TOF) *m/z*: [M + Na]⁺ calculated for C₃₃H₅₈NaO₆Si, 601.3895; found, 601.3894.



Compound S6

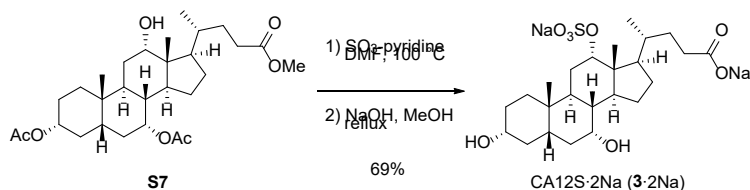
DMAP (21.4 mg, 0.175 mmol) and Ac₂O (465 μ l, 4.92 mmol) were added to a solution of Compound S5 (949 mg, 1.64 mmol) in pyridine (5.3 ml) at 0°C. After being stirred for 23 hours at room temperature, the mixture was diluted with CH₂Cl₂, washed with saturated aqueous CuSO₄ and brine, and dried over Na₂SO₄. After concentration in vacuo, the residue was purified by flash chromatography over silica gel with *n*-hexane–EtOAc (10:1 to 7:1) to yield Compound S6 as a colorless oil (831 mg, 82%): [α]_D²⁵ +38.3 (*c* 0.630, CHCl₃); IR (neat cm⁻¹): 1737 (C=O); ¹H NMR (500 MHz, CDCl₃) δ 0.64 (q, *J* = 8.0 Hz, 6H), 0.64 (s, 3H), 0.92 (s, 3H), 0.95 (d, *J* = 6.3 Hz, 3H), 0.99–1.12 (m, 2H), 1.03 (t, *J* = 8.0 Hz, 9H), 1.19–1.24 (m, 1H), 1.29–1.53 (m, 7H), 1.55–1.63 (m, 3H), 1.69–1.75 (m, 1H), 1.76–1.90 (m, 4H), 1.90–1.96 (m, 1H), 1.96–2.08 (m, 2H), 2.03 (s, 3H), 2.03 (s, 3H), 2.16–2.29 (m, 2H), 2.34–2.40 (m, 1H), 3.67 (s, 3H), 4.05–4.07 (m, 1H), 4.53–4.60 (m, 1H), 4.87–4.90 (m, 1H); ¹³C{¹H} NMR (125 MHz, CDCl₃) δ 5.8 (3C), 7.1 (3C), 12.2, 17.6, 21.4, 21.5, 22.6, 23.4, 26.8, 27.7, 27.8, 28.8, 31.01, 31.04, 31.5, 34.7, 34.78, 34.82, 35.7, 38.4, 41.0, 41.1, 46.1, 47.1, 51.5, 71.2, 73.7, 74.0, 170.4, 170.8, 174.7; HRMS (ESI-TOF) *m/z*: [M + Na]⁺ calculated for C₃₅H₆₀NaO₇Si, 643.4001; found, 643.4002.



Compound S7

To a solution of Compound S6 (831 mg, 1.34 mmol) in THF (22 ml) was added a solution of TBAF (1M in THF 3.35 ml, 3.35 mmol) at 0°C. After constant stirring for 15 hours at room temperature, the mixture was diluted with EtOAc. The whole mixture was washed with saturated aqueous NH₄Cl and brine, and dried over Na₂SO₄. After concentration in vacuo, the residue was purified by flash chromatography over silica gel with *n*-hexane–EtOAc (3:1 to

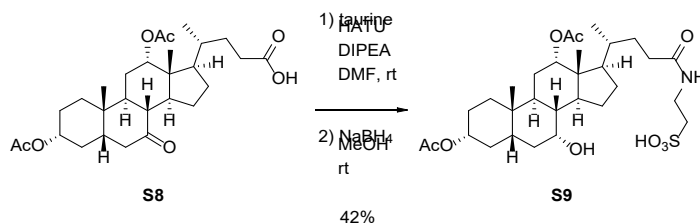
0:100) to yield Compound S7 as a white solid (653 mg, 96%): mp 181–183°C; $[\alpha]^{26}_D +23.5$ (*c* 0.668, CHCl₃); IR (neat cm⁻¹): 3498 (OH), 1725 (C=O); ¹H NMR (500 MHz, CDCl₃) δ 0.69 (s, 3H), 0.92 (s, 3H), 0.98 (d, *J* = 6.3 Hz, 3H), 1.04–1.13 (m, 2H), 1.24–1.54 (m, 8H), 1.55–1.65 (m, 4H), 1.66–1.75 (m, 2H), 1.77–1.90 (m, 4H), 1.95 (ddd, *J* = 15.7, 5.7, 3.4 Hz, 1H), 2.03 (s, 3H), 2.07 (s, 3H), 2.04–2.13 (m, 1H), 2.17–2.27 (m, 2H), 2.38 (ddd, *J* = 15.4, 10.3, 5.1 Hz, 1H), 3.67 (s, 3H), 3.99–4.02 (m, 1H), 4.54–4.62 (m, 1H), 4.87–4.91 (m, 1H); ¹³C {¹H} NMR (125 MHz, CDCl₃) δ 12.5, 17.3, 21.5, 21.6, 22.5, 22.9, 26.6, 27.2, 28.1, 28.5, 30.8, 31.0, 31.2, 34.3, 34.5, 34.7, 34.9, 38.0, 40.9, 42.1, 46.5, 47.1, 51.5, 70.8, 72.7, 74.1, 170.5, 170.7, 174.6; HRMS (ESI-TOF) *m/z*: [M + Na]⁺ calculated for C₂₉H₄₆NaO₇, 529.3136; found, 529.3136.



Disodium cholate 12-sulfate (CA12S·2Na)

By a procedure identical with that described for synthesis of Compound 1·2Na from Compound S1, cholic acid derivative Compound S7 (102 mg, 0.201 mmol) was converted into CA12S·2Na (Compound 3·2Na) as a white amorphous solid (74.3 mg, 69%): mp 195–198°C; $[\alpha]^{25}_D +40.3$ (*c* 0.740, MeOH); IR (neat cm⁻¹): 3383 (OH), 1560 (C=O), 1410 (S=O); ¹H NMR (500 MHz, D₂O) δ 0.76 (s, 3H), 0.92 (s, 3H), 0.96–1.05 (m, 1H), 0.98 (d, *J* = 6.3 Hz, 3H), 1.08–1.19 (m, 1H), 1.24–1.36 (m, 2H), 1.36–1.56 (m, 5H), 1.56–1.73 (m, 5H), 1.74–1.87 (m, 3H), 1.88–1.96 (m, 1H), 1.96–2.06 (m, 2H), 2.07–2.20 (m, 3H), 2.20–2.27 (m, 1H), 3.42–3.50 (m, 1H), 3.87–3.91 (m, 1H), 4.69–4.73 (m, 1H); ¹³C {¹H} NMR (125MHz, D₂O) δ 12.3, 17.7, 22.6, 23.3, 25.1, 27.3, 27.7, 29.9, 32.9, 34.4, 34.9, 35.2, 35.4, 35.9, 39.1, 39.4, 41.6, 42.9, 46.3,

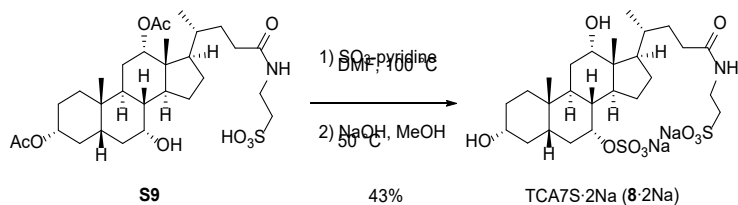
47.1, 69.0, 72.4, 84.1, 185.3; HRMS (ESI-TOF) m/z : $[M + H - 2Na]^-$ calculated for $C_{24}H_{39}O_8S$, 487.2371; found, 487.2378.



Compound S9

Diisopropylethylamine (421 μ l, 2.41 mmol) and HATU (461 mg, 1.21 mmol) were added to a stirred solution of Compound S8 (395 mg, 0.805 mmol) in dry DMF (6.0 ml) at room temperature under an argon atmosphere. After constant stirring for 30 min, taurine (153 mg, 1.22 mmol) was added. The mixture was stirred for 17.5 hours at room temperature. After concentration in vacuo, the residue was diluted with Et₂O and saturated aqueous NaHCO₃. After the aqueous layer was concentrated in vacuo, MeOH was added to the residue and the resulting precipitate was filtered. After the filtrate was concentrated in vacuo, the residue was dissolved in water (3 ml). Using a procedure identical to that described for synthesis of Compound 1 from Compound S1, the aqueous solution of sulfonic acid was purified by Sep-Pak[®] C18 cartridge and lyophilized to yield the taurine-conjugated product as a pale yellow amorphous solid (283 mg), which was used without further purification. MeOH (4.0 ml) and NaBH₄ (34.6 mg, 0.915 mmol) were added to a stirred solution of the taurine-conjugated product (283 mg) at room temperature. After constant stirring for 17.5 hours at this temperature, the mixture was diluted with saturated aqueous NH₄Cl and concentrated in vacuo. The residue was dissolved in CHCl₃. The organic layer was washed with 10% aqueous HCl three times and dried over Na₂SO₄. After concentration in vacuo, the residue was purified by flash

chromatography over silica gel with CHCl₃-MeOH (5:1 to 4:1) to yield Compound S9 as a white solid (203 mg, 42% over two steps). All spectral data were in agreement with previously reported findings (85): ¹H NMR (500 MHz, CD₃OD) δ 0.78 (s, 3H), 0.85 (d, *J* = 6.3 Hz, 3H), 0.94 (s, 3H), 1.00–1.08 (m, 1H), 1.11–1.20 (m, 1H), 1.24–1.48 (m, 7H), 1.49–1.66 (m, 4H), 1.66–1.81 (m, 6H), 1.90–2.00 (m, 2H), 1.99 (s, 3H), 2.05–2.14 (m, 3H), 2.10 (s, 3H), 2.24 (ddd, *J* = 13.7, 10.3, 5.1 Hz, 1H), 2.35–2.41 (m, 1H), 2.96 (t, *J* = 6.9 Hz, 2H), 3.58 (t, *J* = 6.9 Hz, 2H), 3.80–3.83 (m, 1H), 4.47–4.55 (m, 1H), 5.06–5.08 (m, 1H).



Disodium taurocholate 7-sulfate (TCA7S·2Na)

TCA7S·2Na was synthesized by modifying a previously published method (89, 90). To a stirred solution of Compound S9 (80.1mg, 0.134 mmol) in dry DMF (1.6 ml) was added sulfur trioxide-pyridine complex (214 mg, 1.35 mmol) under argon atmosphere. After being stirred for 50 hours at 100°C, the mixture was concentrated in vacuo. A solution of NaOH (0.792 g, 19.8 mmol) in MeOH (16 ml) was added to the mixture. After 45 hours of stirring at 50°C, the mixture was adjusted to pH 8 with 10% aqueous HCl and concentrated in vacuo. MeOH was added to the residue, and the resulting precipitate was filtered. After the filtrate was concentration in vacuo, the residue was dissolved in water (3 ml), which was purified by Sep-Pak[®] C18 cartridge and lyophilized to yield TCA7S·2Na (Compound 8·2Na) as a pale yellow solid (36.8 mg, 43%): mp 186°C (decomp.); [α]_D²⁴ +7.6 (*c* 0.520, MeOH); IR (neat cm⁻¹): 3336 (OH), 1654 (C=O), 1449 (S=O); ¹H NMR (500 MHz, D₂O) δ 0.71 (s, 3H), 0.93 (s, 3H), 0.97 (d, *J* = 6.3 Hz, 3H), 0.99–1.17 (m, 2H), 1.20–1.44 (m, 4H), 1.46–1.53 (m, 1H), 1.55–1.97 (m,

13H), 1.99–2.10 (m, 2H), 2.20 (ddd, $J = 14.1, 7.4, 7.4$ Hz, 1H), 2.31 (ddd, $J = 14.1, 9.7, 5.1$ Hz, 1H), 3.07 (t, $J = 6.9$ Hz, 2H), 3.47–3.53 (m, 1H), 3.56 (t, $J = 6.9$ Hz, 2H), 4.03–4.07 (m, 1H), 4.47–4.51 (m, 1H); $^{13}\text{C}\{^1\text{H}\}$ NMR (125 MHz, D_2O) δ 12.6, 17.3, 22.5, 23.2, 27.6, 27.7, 28.2, 29.8, 31.0, 32.2, 33.4, 34.6, 35.1, 35.4, 35.6, 38.4, 39.4, 41.5, 42.1, 46.7, 47.2, 50.4, 72.2, 73.8, 79.9, 178.16; HRMS (ESI-TOF) m/z : $[\text{M} + \text{H} - 2\text{Na}]^-$ calculated for $\text{C}_{26}\text{H}_{44}\text{O}_{10}\text{NS}_2$, 594.2412; found, 594.2410.

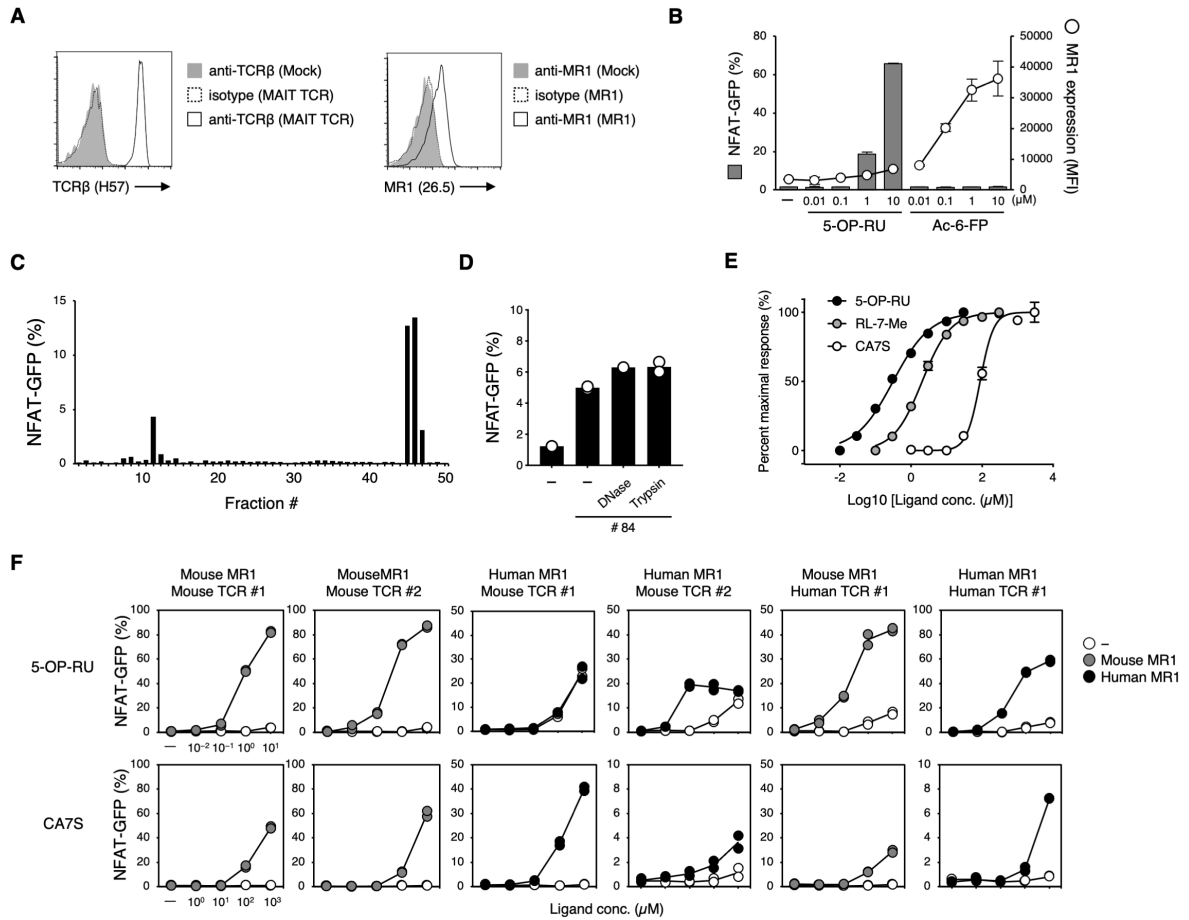


Fig. S1. Purification and characterization of CA7S. (A) A MAIT TCR and MR1 were co-expressed in TCR-deficient T cell hybridoma (81). Surface expression levels of MAIT TCR and MR1 on reporter cells were assessed by surface staining with anti-mouse TCRβ (H57-597) (left) or anti-human/mouse/rat MR1 (26.5) (right). HTK888 and MOPC-173 were used as isotype control Abs, respectively (dotted line). (B) NFAT-GFP reporter cells were stimulated with vehicle control, 5-OP-RU or Ac-6-FP. GFP expression and MR1 surface expression were evaluated at 6 hours after stimulation. Closed columns indicate GFP expression. Open circles indicate MR1 surface expression. (C) Percentages of GFP⁺ cells upon stimulation with the 50 fractions from the secondary purified intestine of SPF mice. (D) Percentages of GFP⁺ cells upon stimulation with DNase or trypsin treated fraction #84. (E) Dose-response curves for 5-OP-RU, RL-7-Me, and CA7S. (F) Combinations of human or mouse MR1 with three clones of MAIT TCR were coexpressed in NFAT-GFP reporter cells. These cells were stimulated with vehicle control, 5-OP-RU, or CA7S and analyzed by flow cytometry after 20 hours. Data are presented as the means ± SD of triplicates (B and E) or individual values of duplicate assays (D and F). All data are representative of more than two independent experiments.

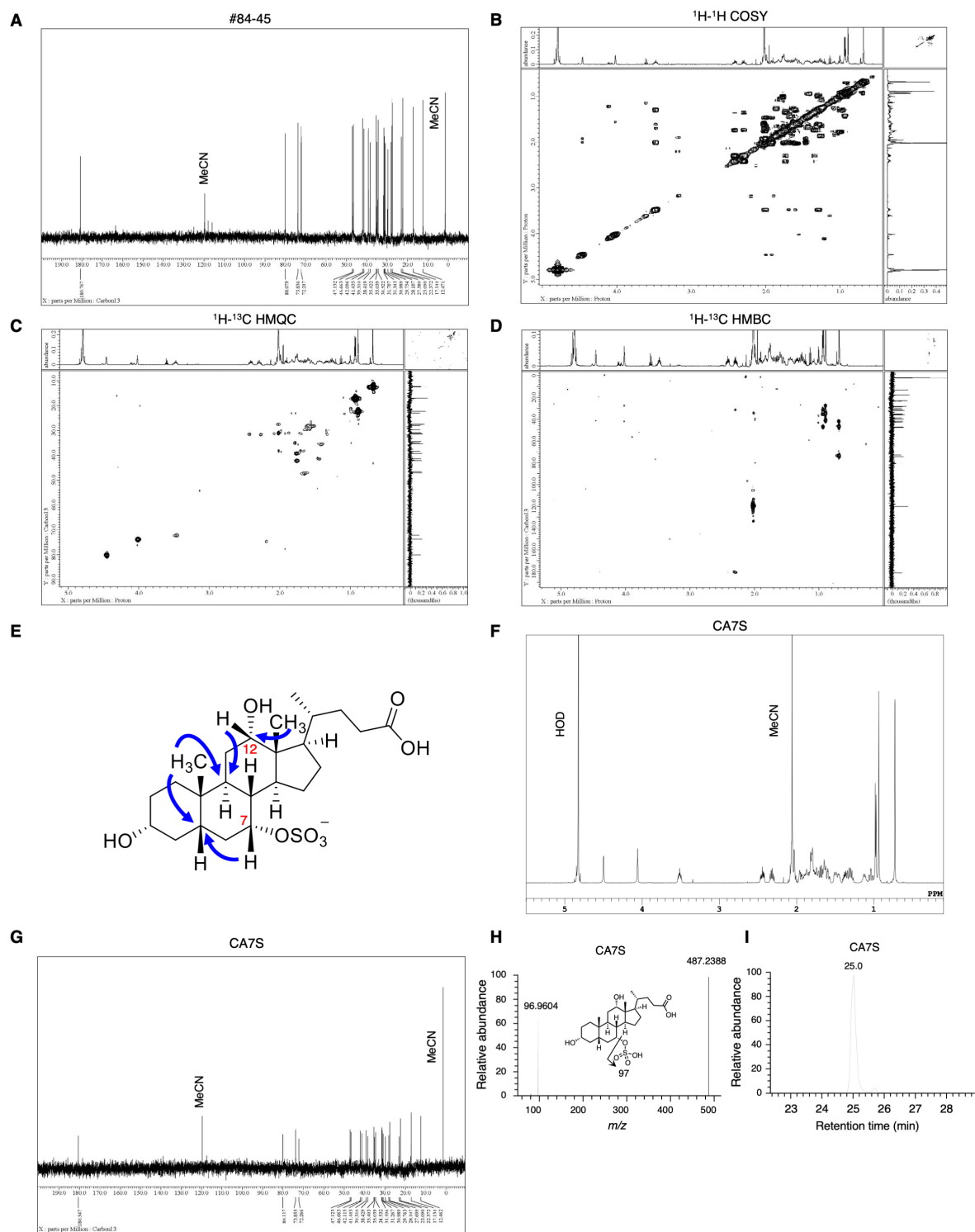


Fig. S2. Structural determination of CA7S. (A) ^{13}C NMR spectra (150 MHz, D_2O) of fraction #84-45. (B to D) 2D NMR analyses, including ^1H - ^1H correlation spectroscopy (COSY) (B), ^1H - ^{13}C heteronuclear multiple quantum correlation spectroscopy (HMQC) (C) and ^1H - ^{13}C heteronuclear multiple-bond correlation spectroscopy (HMBC) (D) of fraction #84-45. (E) Key ^1H - ^{13}C HMBC correlations of fraction #84-45. (F to I) ^1H NMR (600 MHz, D_2O) spectra (F), ^{13}C NMR (150 MHz, D_2O) spectra (G), MS/MS spectra (H), and extracted ion chromatograms (I) of synthetic CA7S.

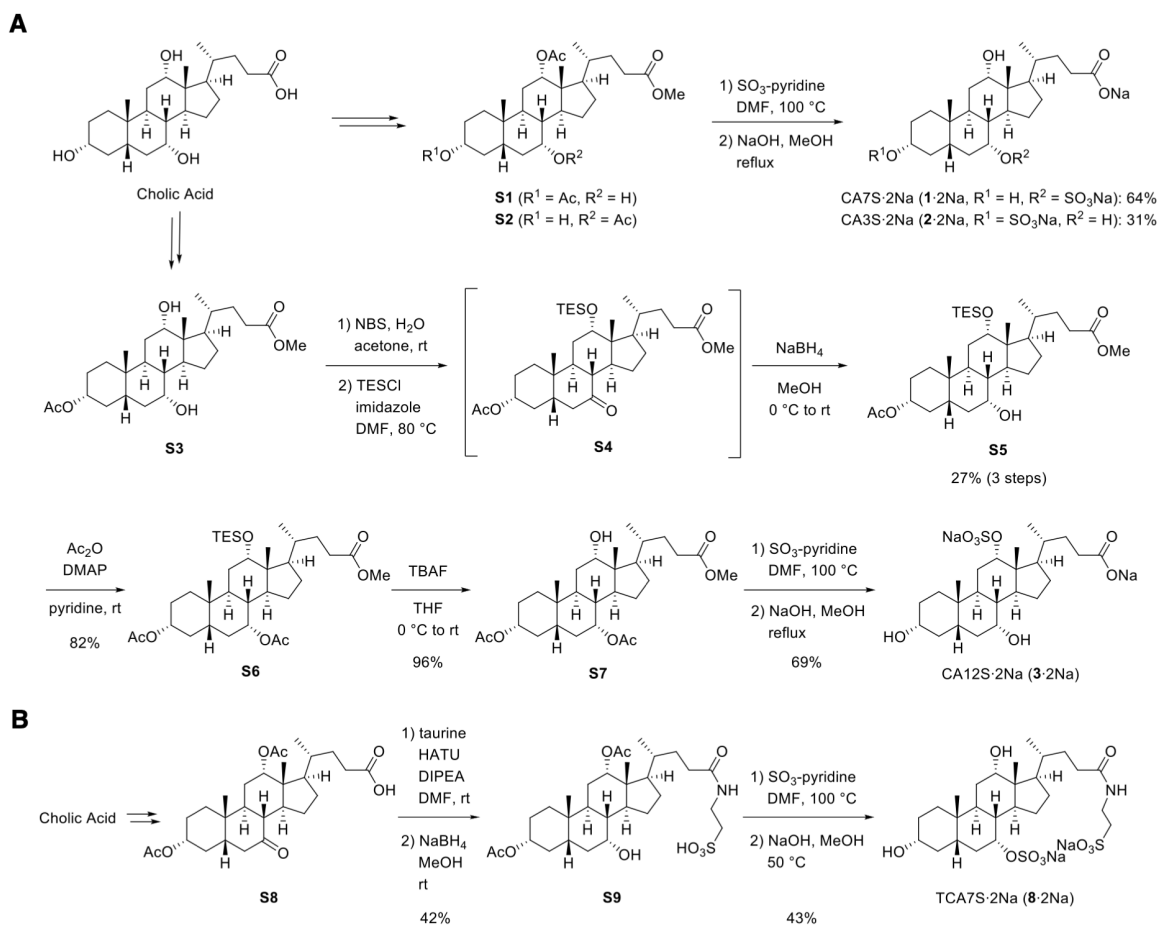


Fig. S3. Chemical synthesis of bile acid metabolites. (A) Synthetic schemes of CA7S (Compound 1), CA3S (Compound 2), and CA12S (Compound 3). (B) Synthetic scheme of TCA7S (Compound 8).

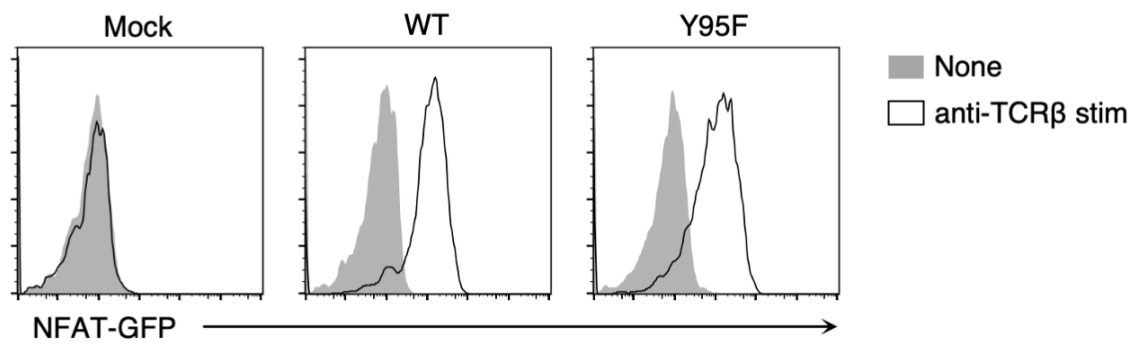


Fig. S4. Stimulation of reporter cells expressing mutant TCR α . Reporter cells were transfected with vector alone (Mock), MAIT TCR β together with WT MAIT TCR α (WT), or mutant TCR α (Y95F). The reporter cells were stimulated with 10 μ g/ml of plate-coated anti-mouse TCR β (H57-597). GFP expression was analyzed by flow cytometry after 20 hours.

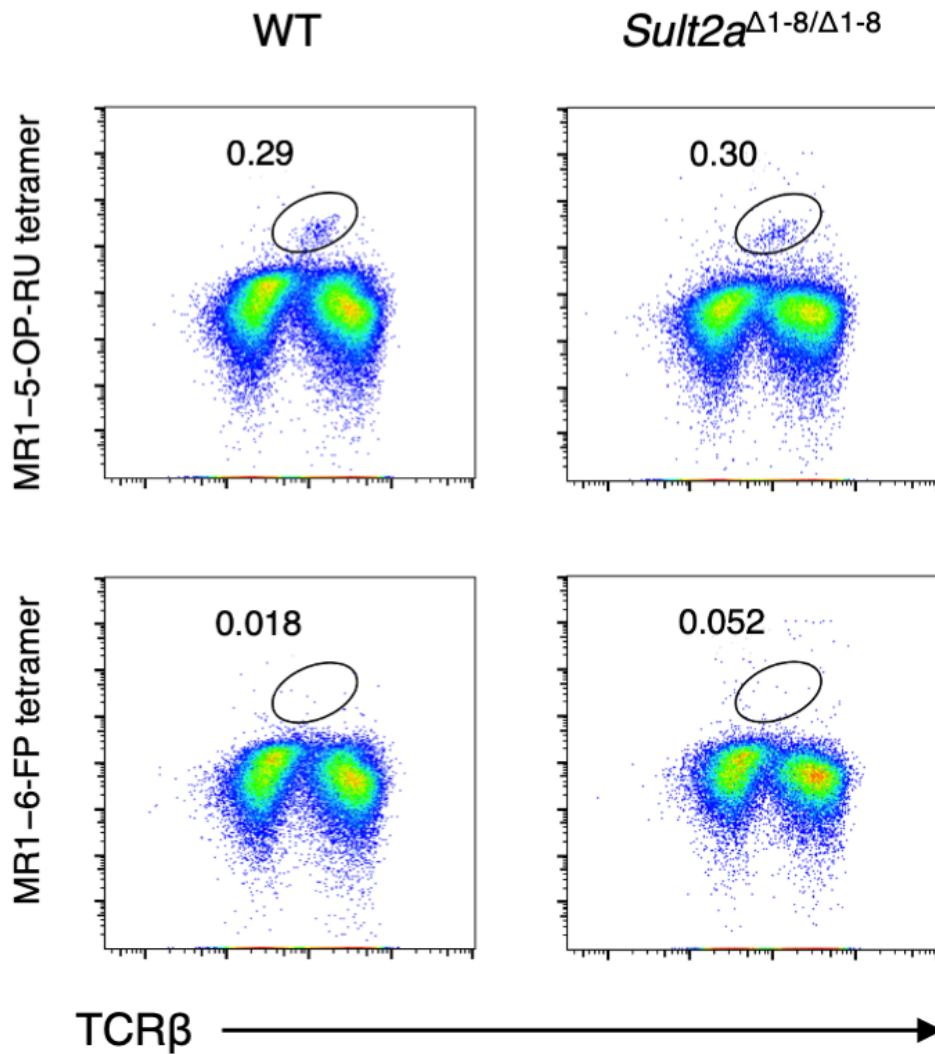


Fig. S5. Liver MAIT cells in *Sult2a*-deficient mice. Representative flow cytometry dot plots of liver CD45⁺CD19⁻TCRβ⁺MR1-5-OP-RU tetramer⁺ MAIT cells from WT or *Sult2a*^{Δ1-8/Δ1-8} mice. MR1-6-FP tetramer staining was used as a negative control for the MR1-5-OP-RU tetramer.

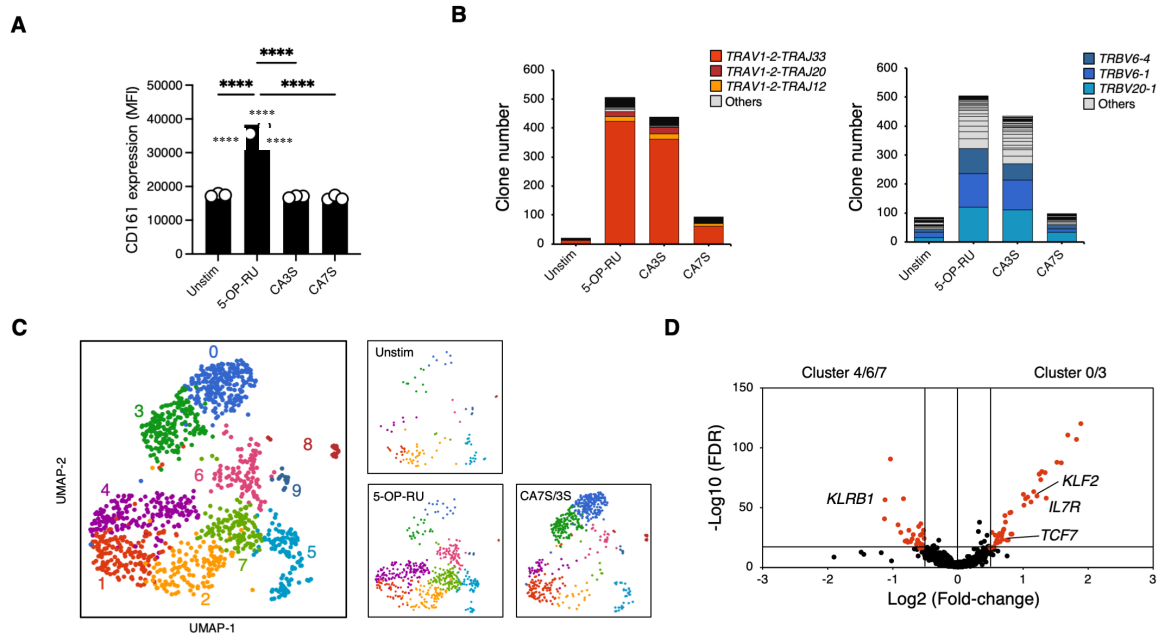


Fig. S6. Responses of human MAIT cells upon stimulation with CAS or 5-OP-RU. (A) CD161 expression (MFI) on CD3⁺CD161⁺MR1 – 5-OP-RU-tetramer⁺ MAIT cells in PBMCs 6 days after stimulation with or without 5-OP-RU, CA3S, or CA7S. **(B to D)** Human PBMCs were stimulated with vehicle control (Unstim), 5-OP-RU (10 μM), CA3S (500 μM), or CA7S (500 μM) for 17 days. **(B)** TCRαβ usage of CD3⁺CD161⁺MR1–5-OP-RU tetramer⁺ cells for each stimulus group. Vα-Jα (left) and Vβ (right) are shown. **(C)** UMAP projection based on mRNA expression of all (left) or each stimulus group (Unstim, 5-OP-RU, or CA7S/3S, right) **(D)** Volcano plot of mRNA expression comparing the characteristic clusters of **(A)** 5-OP-RU stimulation (cluster 4/6/7) and CA7S/3S stimulation (cluster 0/3). Data are presented as individual values and the means of triplicate assays. *****P*<0.001, by two-tailed, one-way ANOVA followed by Tukey’s multiple comparison test.

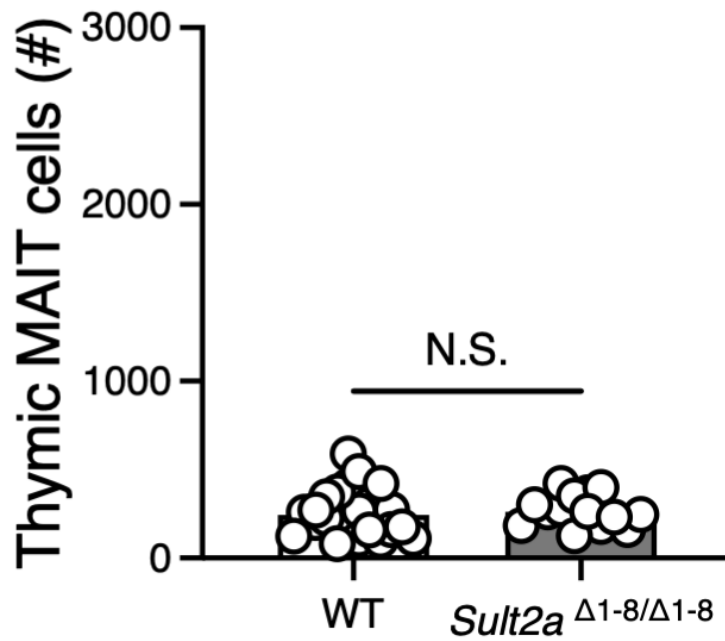


Fig. S7. Thymic MAIT cells in *Sult2a*^{Δ1-8/Δ1-8} mice under germ-free conditions. Germ-free *Sult2a*^{Δ1-8/Δ1-8} mice were rederived by in vitro fertilization. Thymic MAIT cells from 8-week-old WT and *Sult2a*^{Δ1-8/Δ1-8} mice under germ-free conditions were analyzed by tetramer staining as described in Fig. 6A. Data are from experiments with 14 or more mice per group. Each symbol indicates individual mice. N.S., not significant.

A

1st purify conditions			
Column	COSMOSIL PBr 4.6mm I.D. x 250mm		
Eluent A	A: water (0.1%TFA)		
Eluent B	B: AcCN: water = 80:20 (0.1%TFA)		
Flow Rate	1.0mL/min gradient		
Column Temperature	R.T.		
Fractionation	0.5mL/Fr		
	Time (min)	A (%)	B (%)
Gradient Condition	0	100	0
	7	100	0
	55	0	100
	60	0	100
	62	100	0
	65	stop	

B

2nd purify conditions			
Column	TSKgel Amide-80 5 μ m 4.6mm I.D. x 250mm		
Eluent A	A: water (0.1%TFA)		
Eluent B	B: AcCN (0.1%TFA)		
Flow Rate	1.0mL/min gradient		
Column Temperature	R.T.		
Fractionation	0.5mL/Fr		
	Time (min)	A (%)	B (%)
Gradient Condition	0	0	95
	7	0	95
	55	100	0
	60	100	0
	62	0	100
	65	stop	

Table S1. HPLC conditions for purification. (A and B) HPLC conditions for (A) the primary purification on reversed-phase column chromatography and (B) the secondary purification on hydrophilic interaction chromatography (HILIC).

	CA3S	CA12S
Tissue	Average \pm SD (pmol/mg)	
Thymus	N.D.	N.D.
Liver	N.D.	N.D.
Gallbladder	N.D.	N.D.
Duodenum	N.D.	N.D.
Jejunum	N.D.	N.D.
Ileum	N.D.	N.D.
Cecum	N.D.	N.D.
Colon	N.D.	N.D.

Table S2. Quantitative determination of CA3S and CA12S in mouse tissues. Tissue distribution of CA3S and CA12S in various tissues of SPF mice. Data are presented as the means \pm SD from experiments with three mice per group and are representative of two independent experiments. N.D., not detected.

Cluster 1			
Name	ES	p-value	FDR
Innate immune response	-0.67865	0.001	0.04724
Defense response to other organism	-0.67095	0.001	0.04724
Response to cytokine	-0.62764	0.001	0.04724
Defense response	-0.60893	0.001	0.04724
Positive regulation of immune system process	-0.53741	0.001	0.04724
Regulation of immune response	-0.51989	0.001	0.04724
Organic acid metabolic process	-0.50649	0.001	0.04724
Regulation of immune system process	-0.50648	0.001	0.04724
Transmembrane transport	-0.50306	0.001	0.04724
Cell cell signaling	-0.4987	0.001	0.04724
Protein localization to organelle	-0.49436	0.001	0.04724
Proteolysis	-0.48758	0.001	0.04724
Mrna metabolic process	-0.4786	0.001	0.04724
Exocytosis	-0.47674	0.001	0.04724
Regulation of protein localization	-0.47035	0.001	0.04724
Cellular protein catabolic process	-0.47031	0.001	0.04724
Secretion	-0.4668	0.001	0.04724
Protein modification by small protein conjugation	-0.46519	0.001	0.04724
Regulation of cell death	-0.46224	0.001	0.04724
Protein catabolic process	-0.46132	0.001	0.04724
Cellular macromolecule catabolic process	-0.44836	0.001	0.04724
Intracellular protein transport	-0.4478	0.001	0.04724
Organonitrogen compound catabolic process	-0.44531	0.001	0.04724
Positive regulation of molecular function	-0.43894	0.001	0.04724
Intracellular transport	-0.43225	0.001	0.04724

Cluster 0			
Name	ES	p-value	FDR
Positive regulation of vascular wound healing	0.99986	0.00202	0.06026
Negative regulation of toll like receptor 4 signaling pathway	0.97634	0.00225	0.0605
Negative regulation of t cell mediated cytotoxicity	0.96164	0.00244	0.0605
Acylglycerol homeostasis	0.93427	0.00244	0.0605
Adenylyl cyclase activating adrenergic receptor signaling pathway involved in heart process	0.94884	0.00244	0.0605
Negative regulation of interleukin 8 secretion	0.93358	0.00244	0.0605
G protein coupled receptor signaling pathway involved in heart process	0.94897	0.00252	0.06105
Histone h3 k14 acetylation	0.84244	0.00261	0.06156
Actin filament severing	0.86	0.00261	0.06156
Regulation of aspartic type endopeptidase activity involved in amyloid precursor protein catabolic process	0.8468	0.00261	0.06156
Negative regulation of p38mapk cascade	0.85534	0.00261	0.06156
Negative regulation of microglial cell activation	0.90483	0.00261	0.06156
Negative regulation of macrophage activation	0.86433	0.00269	0.06246
Detection of mechanical stimulus	0.85941	0.00269	0.06246
Angiogenesis involved in wound healing	0.89993	0.00269	0.06246
Neutrophil extravasation	0.85242	0.00269	0.06246
Regulation of cell cell adhesion mediated by integrin	0.82478	0.00272	0.06268
Regulation of toll like receptor 4 signaling pathway	0.89975	0.00272	0.06268
Negative regulation of smoothened signaling pathway	0.81159	0.00277	0.06326
Negative regulation of camp mediated signaling	0.85076	0.00292	0.06519
V d j recombination	0.86972	0.00296	0.06534
Forebrain cell migration	0.84898	0.00337	0.06795
Positive regulation of wound healing	0.75979	0.00337	0.06795
Negative regulation of g protein coupled receptor signaling pathway	0.71663	0.00342	0.06825
Positive regulation of response to wounding	0.73368	0.00342	0.06825

Table S3. Gene ontology upon stimulation with CA7S or 5-OP-RU. Top 25 gene ontology terms of biological processes based on differentially expressed genes comparing the characteristic clusters of 5-OP-RU stimulation (cluster 1, left) and CA7S stimulation (cluster 0, right), related to Fig. 7, D and E. Inflammatory (cluster 1) and tissue repair/wound healing-related (cluster 0) gene ontology terms are both shown in bold.

Data S1. Chemical information of targeted bile acids.